

REPORT DOCUMENTATION PAGE				Form Approved OMB No. 0704-0188	
Public reporting burden for this collection of information is estimated to average 1 hour per response, including the time for reviewing instructions, searching existing data sources, gathering and maintaining the data needed, and completing and reviewing this collection of information. Send comments regarding this burden estimate or any other aspect of this collection of information, including suggestions for reducing this burden to Department of Defense, Washington Headquarters Services, Directorate for Information Operations and Reports (0704-0188), 1215 Jefferson Davis Highway, Suite 1204, Arlington, VA 22202-4302. Respondents should be aware that notwithstanding any other provision of law, no person shall be subject to any penalty for failing to comply with a collection of information if it does not display a currently valid OMB control number. PLEASE DO NOT RETURN YOUR FORM TO THE ABOVE ADDRESS.					
1. REPORT DATE (DD-MM-YYYY) 25-02-2008		2. REPORT TYPE Journal Article		3. DATES COVERED (From - To)	
4. TITLE AND SUBTITLE Standardization of Hall Thruster Efficiency Analysis: Methodology and Historical Perspective (Preprint)				5a. CONTRACT NUMBER	
				5b. GRANT NUMBER	
				5c. PROGRAM ELEMENT NUMBER	
6. AUTHOR(S) Daniel L. Brown (ERC); C. William Larson & William A. Hargus, Jr. (AFRL/RZSS)				5d. PROJECT NUMBER	
				5e. TASK NUMBER 33SP0706	
				5f. WORK UNIT NUMBER	
7. PERFORMING ORGANIZATION NAME(S) AND ADDRESS(ES) Air Force Research Laboratory (AFMC) AFRL/RZSS 1 Ara Drive Edwards AFB CA 93524-7013				8. PERFORMING ORGANIZATION REPORT NUMBER AFRL-RZ-ED-JA-2008-112	
9. SPONSORING / MONITORING AGENCY NAME(S) AND ADDRESS(ES) Air Force Research Laboratory (AFMC) AFRL/RZS 5 Pollux Drive Edwards AFB CA 93524-7048				10. SPONSOR/MONITOR'S ACRONYM(S)	
				11. SPONSOR/MONITOR'S NUMBER(S) AFRL-PR-ED-JA-2008-112	
12. DISTRIBUTION / AVAILABILITY STATEMENT Approved for public release; distribution unlimited (PA #08148A).					
13. SUPPLEMENTARY NOTES Submitted for publication in AIAA Journal.					
14. ABSTRACT The rocket power efficiency equation was analytically decomposed to explicitly account for the effects of energy conversion losses, plume divergence, and the velocity distribution function of the propellant jet. In this approach, thruster efficiency is the product of (1) energy efficiency and (2) propellant utilization efficiency. Energy efficiency is expressed as the product of voltage utilization efficiency and current utilization efficiency, and incorporates losses from Joule heating, radiation, and ionization processes. Energy efficiency contains no information about the vector properties of the jet. Propellant utilization efficiency incorporates losses from plume divergence and ion jet composition, and is unity for 100% ionization to a single ion species whose velocity vectors are directed along the thrust axis. The efficiency architecture is derived from first principles and is applicable to all propulsion employing electrostatic acceleration, including Hall thrusters and ion engines. The analysis is compared to past methodologies and is illustrated with thrust and far-field plume measurements of a laboratory Hall thruster.					
15. SUBJECT TERMS					
16. SECURITY CLASSIFICATION OF:			17. LIMITATION OF ABSTRACT SAR	18. NUMBER OF PAGES 27	19a. NAME OF RESPONSIBLE PERSON Dr. William A. Hargus, Jr.
a. REPORT Unclassified	b. ABSTRACT Unclassified	c. THIS PAGE Unclassified			19b. TELEPHONE NUMBER (include area code) N/A

Standardization of Hall Thruster Efficiency Analysis: Methodology and Historical Perspective (Preprint)

Daniel L. Brown¹, C. William Larson², William A. Hargus, Jr.³
Air Force Research Laboratory, Edwards AFB, CA 93524-7680

and

Alec D. Gallimore⁴
*Plasmadynamics and Electric Propulsion Laboratory
University of Michigan, Ann Arbor, MI, 48109, USA*

[Abstract] The rocket power efficiency equation was analytically decomposed to explicitly account for the effects of energy conversion losses, plume divergence, and the velocity distribution function of the propellant jet. In this approach, thruster efficiency is the product of (1) energy efficiency and (2) propellant utilization efficiency. Energy efficiency is expressed as the product of voltage utilization efficiency and current utilization efficiency, and incorporates losses from Joule heating, radiation, and ionization processes. Energy efficiency contains no information about the vector properties of the jet. Propellant utilization efficiency incorporates losses from plume divergence and ion jet composition, and is unity for 100% ionization to a single ion species whose velocity vectors are directed along the thrust axis. The efficiency architecture is derived from first principles and is applicable to all propulsion employing electrostatic acceleration, including Hall thrusters and ion engines. The analysis is compared to past methodologies and is illustrated with thrust and far-field plume measurements of a laboratory Hall thruster.

Distribution A – Approved for Public Release, Distribution Unlimited.

¹ Research Scientist, ERC Inc.; Ph.D. Candidate, University of Michigan, Plasmadynamics and Electric Propulsion Laboratory; Daniel.Brown@edwards.af.mil. AIAA Student Member.

² Research Scientist, Spacecraft Propulsion Branch, AFRL/RZSS; Carl.Larson@edwards.af.mil. AIAA Senior Member.

³ Research Scientist, Spacecraft Propulsion Branch, AFRL/RZSS; William.Hargus@edwards.af.mil. AIAA Senior Member.

⁴ Laboratory Director, Plasmadynamics and Electric Propulsion Laboratory; Professor, Department of Aerospace Engineering; Associate Dean, Horace H. Rackham School of Graduate Studies, Associate Fellow AIAA.)

Nomenclature

E_1	= voltage exchange parameter = $\frac{1}{2}(\mathbf{T}/\dot{m})^2/(V_a \mathcal{F}/\mathcal{M}) = \Phi(1-\beta)\chi$
E_2	= mass exchange parameter = $(\dot{m}/I_a)(\mathcal{F}/\mathcal{M}) = (1-r)/\chi$
f_0, f_1, f_2, f_3	= exit mass fractions of $\text{Xe}^0, \text{Xe}^{+1}, \text{Xe}^{+2}, \text{Xe}^{+3}$, where $f_0 + f_1 + f_2 + f_3 = 1$
f_i	= ion mass fraction at exit = $f_1 + f_2 + f_3$
f_1^*, f_2^*, f_3^*	= reduced ion mass fractions at exit, $f_1^* + f_2^* + f_3^* = 1$, where $f_1^* = f_1/f_i, f_2^* = f_2/f_i, f_3^* = f_3/f_i$
\mathcal{F}	= Faraday constant, 96,485 coulombs/mol of charge
$f(\mathbf{v})$	= velocity distribution function of ions and neutrals
g_0	= Earth's gravitational constant at sea level, 9.806 m/s ²
I_a	= anode discharge current
I_{Beam}	= integrated beam current = $f_i Q \dot{m} (\mathcal{F}/\mathcal{M})$
I_{Axial}	= integrated axial beam current
I_{sp}	= specific impulse, independent of unit system, $I_{\text{sp}} = \mathbf{T} / \dot{m}$
j	= charge density in the plume measured from a Faraday probe, A/sr
\dot{m}	= anode propellant mass flow rate
\mathcal{M}	= molecular weight of propellant (xenon = 0.1313 kg/mol)
P_{in}	= input power to anode = $V_a I_a$
P_{jet}	= jet power
Q	= average charge of propellant ions in a trimodal jet = $f_1^* + 2f_2^* + 3f_3^*$
q	= unit of charge, 1.609×10^{-19} Coulombs
r	= fractional anode electron current, electron recycle fraction
$(1-r)$	= fractional ion beam current, current utilization efficiency = I_{Beam} / I_a
r_{min}	= minimum fraction of electron current required to sustain discharge
\mathbf{T}	= thrust
V_a	= applied anode potential
$\mathbf{v}_0, \mathbf{v}_1, \mathbf{v}_2, \mathbf{v}_3$	= exit velocities of $\text{Xe}^0, \text{Xe}^{+1}, \text{Xe}^{+2}, \text{Xe}^{+3}$
\mathbf{v}	= exit velocity of ions and neutrals
\mathbf{v}_{ions}	= exit velocity of ions
$\mathbf{y}_0, \mathbf{y}_1, \mathbf{y}_2, \mathbf{y}_3$	= reduced velocity ratios, where $\mathbf{y}_0 = \mathbf{v}_0/ \mathbf{v}_1 , \mathbf{y}_1 = \mathbf{v}_1/ \mathbf{v}_1 , \mathbf{y}_2 = \mathbf{v}_2/ \mathbf{v}_1 , \mathbf{y}_3 = \mathbf{v}_3/ \mathbf{v}_1 $
α	= indicator of the 'quality' of ionization in $\Phi_{\text{VDF}}, \alpha = \Phi_{\text{VDF}}/f_i \approx 1.10-0.10Q$
γ	= relationship between particle momentum and current at azimuthal position $\theta, \gamma \approx (\alpha/Q)^{1/2}$
β	= fractional loss of acceleration voltage
$(1-\beta)$	= voltage utilization efficiency = $\Delta V / V_a$
ΔV	= average ion acceleration voltage = $(f_1^* \delta V_1 + 2f_2^* \delta V_2 + 3f_3^* \delta V_3) / Q$
$\delta V_1, \delta V_2, \delta V_3$	= acceleration potential of $\text{Xe}^{+1}, \text{Xe}^{+2}, \text{Xe}^{+3}$
$\varepsilon_1, \varepsilon_2, \varepsilon_3$	= ionization potential of $\text{Xe}^{+1}, \text{Xe}^{+2}, \text{Xe}^{+3}$ (12, 33, 65 eV from neutral ground state)
η_{energy}	= energy efficiency = $P_{\text{jet}}/P_{\text{in}}$
η_{thrust}	= experimental thruster efficiency
θ	= azimuthal position from thruster centerline, $\theta=0^\circ$ on thrust axis
λ	= plume momentum divergence half-angle, $\lambda=0^\circ$ on thrust axis
Φ	= propellant utilization efficiency, $\Phi = \Phi_{\text{VDF}} \Phi_{\text{DIV}}$
Φ_{VDF}	= velocity distribution loss component of propellant utilization, $\Phi_{\text{VDF}} = \alpha f_i$
Φ_{DIV}	= divergence loss component of propellant utilization, $\Phi_{\text{DIV}} = \langle \cos(\theta) \rangle_{mv}^2 \approx \langle \cos(\theta) \rangle_j^2$
χ	= output moles of charge per input moles of propellant, average particle charge = $f_i Q$
$\langle \rangle_m$	= mass weighted average quantity in the plume ($-\pi/2 < \theta < \pi/2$)
$\langle \rangle_{mv}$	= momentum weighted average quantity in the plume ($-\pi/2 < \theta < \pi/2$)
$\langle \rangle_j$	= charge flux weighted average quantity in the plume ($-\pi/2 < \theta < \pi/2$)
(θ)	= variable evaluated at azimuthal position θ , units of sr ⁻¹
z	= ion charge state = 1, 2, 3 for $\text{Xe}^{+1}, \text{Xe}^{+2}, \text{Xe}^{+3}$

Introduction

Standardization of experimental methods, facilities, and apparatus in the electric propulsion community has previously been proposed.¹ A standard approach to Hall thruster efficiency analysis is also necessary to enable consistent comparisons of thruster performance. Present Hall thruster performance models arbitrarily set the anode efficiency equal to the product of several utilization efficiencies, including combinations of current, voltage, charge, mass, and propellant utilization.^{2,3,4,5} This method will often successfully interpret experimental measurements, but it is not based on first principles and there is no assurance that it accurately interprets global plasma properties or relevant loss mechanisms.

A standard, logical architecture is necessary for the analysis of Hall thruster performance data, telemetry (V_a , I_a , and \dot{m}), and plume measurements that is based on a consistent set of definitions, energy conservation, and Newton's Second Law. In electrostatic propulsion, thrust is the result of the utilization of propellant, applied acceleration potential, and discharge current. It is therefore reasonable to express thrust efficiency as a product of the utilization of these three elements.

In this paper, a Hall thruster performance model is derived by analytical separation of thrust efficiency into the product of energy efficiency and propellant utilization efficiency, which are less than unity under all operating conditions. This simple framework reconciles various usages of propellant utilization and exposes the distinction between energy efficiency and thrust efficiency. Energy efficiency is expressed as a product of voltage and current utilization efficiencies, and is rigorously separated from losses associated with the jet vector properties. The model accounts for the effects of the ion velocity distribution function (VDF), ionization fraction, multiply charged ion species, electron recycle fraction, momentum plume divergence, and the loss of acceleration potential within the discharge chamber.

The proposed efficiency architecture is compared to past methodologies, with a historical perspective of early ion engine analyses and similar efforts from the former Soviet Union. To illustrate the fidelity of the proposed analytical model and to demonstrate the utility of various diagnostics in determining Hall thruster utilization efficiencies, experimental performance and plume measurements from a single operating condition of a laboratory Hall thruster is presented. The nature of analytical factorization allows for the characterization of loss mechanisms and interpretation of causal plasma phenomena, but does not account for parasitic losses such as cathode flow and magnet power.

Historical Perspective and Recent Efforts

Investigations of ion acceleration and electron transport using Hall thruster technology began in the early 1960s in the United States and former Soviet Union.^{6,7,8,9,10,11,12,13,14,15,16} The focus of US electric propulsion research shifted primarily to ion engine technology in the early 1970s¹⁷, whereas investigations in the USSR continued Hall thruster advancements throughout the following decades.^{18,19,20}

Analytical factorization of ion engine thruster efficiency was described as early as 1975 by Masek *et al.* in a review of ion engine performance.²¹ Thrust efficiency was factored into the product of energy efficiency and propellant utilization efficiency using Newton's Second Law, with terms accounting for losses due to multiply charged ions and beam divergence. However, the derivation was condensed and justification for treatment of beam divergence and multiply charged ions was not presented. The methodology was not adopted or cited in the ion engine community and is absent in modern analysis.

In the 1990s, the manifestation of Russian Hall thruster technology in the Western spacecraft community catalyzed a resurgence of Hall thruster research.^{22,23,24,25,26,27} Technology transfer that began in the early 1990s brought invaluable benefits and advancements to Western Hall thruster development, but much of the earlier Soviet progress in Hall thruster research that was published in the Russian language was not translated. The limited availability of translated documents from this extensive literature inevitably impeded the transmission of knowledge and progress. As a result, several important contributions from Russian research have not been widely disseminated in the West, including the analytical factorization of thruster efficiency.

Factorization of Hall thruster efficiency was outlined in a manual on stationary plasma engines by Belan, Kim, Oranskiy, and Tikhononv from the Kharkov Aviation Institute in 1989.²⁸ This seminal document was later referenced and the performance methodology summarized by Bugrova *et al.* without explicitly stating the nature of the earlier derivation.²⁹ Kim's highly cited 1998 paper on processes that determine Hall thruster efficiency³⁰ and other contemporary publications^{31,32,33} continued the elaboration of the Kharkov Aviation Institute methodology. These approaches showed similarities to the analysis presented here, and demonstrated relationships between experimental variables and plasma phenomena that affect thruster performance. Over time, factorized performance analyses were substituted with thruster anode efficiency as the product of appointed utilization efficiencies that capture Hall thruster losses as a function of various physical processes with varying levels of completeness.^{2,3,4,5,28-34,}

35,36,37,38

A textbook by Grishin and Leskov analyzed thruster performance based on energy efficiency and thrust efficiency.³⁸ The ratio of thrust efficiency to energy efficiency was asserted to describe the velocity dispersion in magnitude and direction. This ratio will be derived from first principles in the following section, where it will become apparent that the ratio is equivalent to propellant utilization efficiency, which captures losses resulting from plume divergence, incomplete ionization, and the production of multiply charged ions.

The term *propellant utilization efficiency* has been used in at least three different ways in the literature. Most commonly as (1) the ionization fraction, but also as (2) the fraction of momentum carried by ions¹⁸, or as (3) the ratio of output moles of charge to the input moles of propellant³⁹, which is equivalent to the product of the ionization fraction and average ion charge. While the definitions of voltage and current utilization are more standardized, a consistent description of propellant utilization has not emerged. It is apparent that a standard analytical approach is needed to reconcile the terminology.

The analysis of voltage utilization and current utilization have been adopted in several performance models, but reduced acceleration potential and recycled electron current have not been associated with energy efficiency. Recycled electrons, also known as backflow electrons or anode electron current, were characterized as a dominant loss mechanism in the 1960s.¹² Hruby *et al.* quantified electron recycle fraction as a loss in current utilization efficiency, and accounted for loss of acceleration potential in terms of reduced voltage utilization efficiency.⁵ A methodical efficiency analysis by Hofer and Gallimore added terms to account for the utilization of mass and charge.² Several other studies adopted this approach and expanded the analysis to include factors accounting for plume divergence and dispersion of the jet VDF.^{3,40,41} These and other recent formulations of utilization efficiencies do not establish their connection to fundamental conservation principles and Newton's second law, although in some instances the product of terms is remarkably close to the product of the three utilizations set forth in this paper.

Decoupling Energy Efficiency and Propellant Utilization

Using Newton's Second Law, steady state thrust is defined in Eq. (1) as the total axial momentum along thruster centerline. Thrust may be factored into the product of total mass flow, mass weighted average velocity, and momentum weighted average divergence using the definitions shown in Eq. (2), (3), (4), and (5).

$$\mathbf{T} = -\pi \int_{-\pi/2}^{\pi/2} \dot{m}(\theta) \bar{\mathbf{v}}(\theta) \cos(\theta) \sin(\theta) d\theta = -\dot{m} < \bar{\mathbf{v}} >_m < \cos(\theta) >_{mv} \quad (1)$$

where, by definition

$$\dot{m} = \pi \int_{-\pi/2}^{\pi/2} \dot{m}(\theta) \sin(\theta) d\theta \quad (2)$$

$$\bar{\mathbf{v}} = \int_{-\infty}^{+\infty} \mathbf{v} f(\mathbf{v}) d\mathbf{v} / \int_{-\infty}^{+\infty} f(\mathbf{v}) d\mathbf{v} \quad (3)$$

$$< \bar{\mathbf{v}} >_m = \frac{\pi \int_{-\pi/2}^{\pi/2} \dot{m}(\theta) \bar{\mathbf{v}}(\theta) \sin(\theta) d\theta}{\pi \int_{-\pi/2}^{\pi/2} \dot{m}(\theta) \sin(\theta) d\theta} = \frac{\pi \int_{-\pi/2}^{\pi/2} \dot{m}(\theta) \bar{\mathbf{v}}(\theta) \sin(\theta) d\theta}{\dot{m}} \quad (4)$$

$$< \cos(\theta) >_{mv} = \frac{\pi \int_{-\pi/2}^{\pi/2} \dot{m}(\theta) \bar{\mathbf{v}}(\theta) \cos(\theta) \sin(\theta) d\theta}{\pi \int_{-\pi/2}^{\pi/2} \dot{m}(\theta) \bar{\mathbf{v}}(\theta) \sin(\theta) d\theta} = \frac{\pi \int_{-\pi/2}^{\pi/2} \dot{m}(\theta) \bar{\mathbf{v}}(\theta) \cos(\theta) \sin(\theta) d\theta}{\dot{m} < \bar{\mathbf{v}} >_m} \quad (5)$$

The term $\bar{\mathbf{v}}$, as defined in Eq. (3), is the integral over all velocity space of the VDF at azimuthal position θ . All quantities are assumed steady state and evaluated at constant radius from the exit plane, such that the quantities to be integrated have units of sr^{-1} .

Anode efficiency is expressed in terms of thruster telemetry and measured thrust as shown in Eq. (6).

$$\eta_{\text{thrust}} = \frac{\frac{1}{2} \mathbf{T}^2}{\dot{m} P_{\text{in}}} = \frac{\frac{1}{2} \left(\dot{m} < \bar{\mathbf{v}} >_m < \cos(\theta) >_{mv} \right)^2}{\dot{m} P_{\text{in}}} \quad (6)$$

Further analysis of thrust efficiency reveals its relationship to energy efficiency and provides insight into loss mechanisms in Hall thruster performance. In Eq. (7) and (8), thrust efficiency is separated into the product of

energy efficiency and propellant utilization using the definition of jet kinetic energy ($P_{\text{jet}} = \frac{1}{2} \dot{m} \langle \mathbf{v}^2 \rangle_m$), Newton's Second Law, and the mass weighted average squared velocity as defined in Eq. (10).

$$\eta_{\text{thrust}} = \frac{\frac{1}{2} \dot{m} \left(\langle \bar{\mathbf{v}} \rangle_m \langle \cos(\theta) \rangle_{mv} \right)^2}{I_a V_a} \frac{\langle \bar{\mathbf{v}}^2 \rangle_m}{\langle \bar{\mathbf{v}}^2 \rangle_m} = \left(\frac{\left(\langle \bar{\mathbf{v}} \rangle_m \langle \cos(\theta) \rangle_{mv} \right)^2}{\langle \bar{\mathbf{v}}^2 \rangle_m} \right) \left(\frac{\frac{1}{2} \dot{m} \langle \bar{\mathbf{v}}^2 \rangle_m}{I_a V_a} \right) \quad (7)$$

$$\eta_{\text{thrust}} = \left(\frac{\left(\langle \bar{\mathbf{v}} \rangle_m \langle \cos(\theta) \rangle_{mv} \right)^2}{\langle \bar{\mathbf{v}}^2 \rangle_m} \right) \left(\frac{P_{\text{jet}}}{P_{\text{in}}} \right) = \Phi \eta_{\text{energy}} \quad (8)$$

where, by definition

$$\bar{\mathbf{v}}^2 = \frac{\int_{-\infty}^{+\infty} \mathbf{v}^2 f(\mathbf{v}) d\mathbf{v}}{\int_{-\infty}^{+\infty} f(\mathbf{v}) d\mathbf{v}} \quad (9)$$

$$\langle \bar{\mathbf{v}}^2 \rangle_m = \frac{\pi \int_{-\pi/2}^{\pi/2} \dot{m}(\theta) \bar{\mathbf{v}}^2(\theta) \sin(\theta) d\theta}{\pi \int_{-\pi/2}^{\pi/2} \dot{m}(\theta) \sin(\theta) d\theta} = \frac{\pi \int_{-\pi/2}^{\pi/2} \dot{m}(\theta) \bar{\mathbf{v}}^2(\theta) \sin(\theta) d\theta}{\dot{m}} \quad (10)$$

Energy efficiency as defined in Eq. (11) characterizes the conversion of input anode electrical energy to jet kinetic energy, and contains all information about losses that ultimately appear as Joule heating of the thruster, radiation from the jet, and frozen ionization losses in the plume.

$$\eta_{\text{energy}} = \frac{P_{\text{jet}}}{P_{\text{in}}} = \frac{\frac{1}{2} \dot{m} \langle \bar{\mathbf{v}}^2 \rangle_m}{I_a V_a} \quad (11)$$

The quantity Φ as defined in Eq. (12) is a mathematical relationship between the axial momentum that produces thrust and the jet kinetic energy. It contains all loss information associated with the jet vector properties and is unity for 100% ionization to a single ion species where all thrust vectors are directed along the same axis. This ratio, termed propellant utilization efficiency, accounts for losses due to incomplete ionization, plume

divergence and non-uniformity of the VDF that occurs when the jet is composed of multiple ion species with widely varying velocities.

$$\Phi = \frac{\left(\overline{\mathbf{v}}_m \cos(\theta) \right)^2}{\overline{\mathbf{v}^2}_m} = \frac{\overline{\mathbf{v}}_m^2}{\overline{\mathbf{v}^2}_m} \cos^2(\theta) = \Phi_{\text{VDF}} \Phi_{\text{DIV}} \quad (12)$$

For simplicity, the propellant utilization may be factored into two parts. The term Φ_{VDF} is defined in Eq. (13) and quantifies losses from non-uniformity of the VDF that occur when the jet is composed of multiple particle species with widely differing velocities. In Eq. (14), the term Φ_{DIV} quantifies jet momentum losses from plume divergence.

$$\Phi_{\text{VDF}} = \frac{\overline{\mathbf{v}}_m^2}{\overline{\mathbf{v}^2}_m} \quad (13)$$

$$\Phi_{\text{DIV}} = \cos^2(\theta) \quad (14)$$

This formulation is similar to the focusing efficiency from the Kharkov Aviation Institute methodology²⁸, but includes the effects of unionized propellant and differentiates between mass weighted average quantities and momentum weighted average quantities.

Evaluating Velocity Distribution Losses in Propellant Utilization

The influence of non-uniform velocity distribution on propellant utilization is expressed in Eq. (15) using the definitions in Eq. (4) and (10). Knowledge of $f(\mathbf{v})$ throughout the plume is required for a rigorous calculation of this influence in Φ_{VDF} .

$$\Phi_{\text{VDF}} = \frac{\overline{\mathbf{v}}_m^2}{\overline{\mathbf{v}^2}_m} = \frac{\left(\pi \int_{-\pi/2}^{\pi/2} \dot{m}(\theta) \sin(\theta) \overline{\mathbf{v}}(\theta) d\theta \right)^2}{\dot{m} \left(\pi \int_{-\pi/2}^{\pi/2} \dot{m}(\theta) \sin(\theta) \overline{\mathbf{v}^2}(\theta) d\theta \right)} \quad (15)$$

To illustrate the effects of non-uniform VDF, a simple trimodal ion population with neutral xenon is studied. To further simplify, the velocity of the neutrals and each ion species is approximated with a delta function distribution of velocities. This approximation will not significantly affect conclusions that would result from a more complicated model, since each ion species is created within a narrow zone in the channel and the plume is predominantly composed of Xe^{+1} ions. The value of Φ_{VDF} is shown in Eq. (16) for a trimodal ion distribution and evaluated using reduced number fractions and velocity ratios for compact notation. Reduced number fractions are defined according to Eq. (17) and (18) where $f_0^* = f_0/f_i$, $f_1^* = f_1/f_i$, $f_2^* = f_2/f_i$, and $f_3^* = f_3/f_i$. Ratios of velocities of Xe^0 , Xe^{+1} , Xe^{+2} , and Xe^{+3} to the velocity magnitude of Xe^{+1} are defined by $y_0 = v_0/|v_1|$, $y_1 = v_1/|v_1|$, $y_2 = v_2/|v_1|$, $y_3 = v_3/|v_1|$.

$$\Phi_{\text{VDF}} = \frac{\langle \bar{v} \rangle_m^2}{\langle \bar{v}^2 \rangle_m} = \frac{(v_0 f_0 + v_1 f_1 + v_2 f_2 + v_3 f_3)^2}{v_0^2 f_0 + v_1^2 f_1 + v_2^2 f_2 + v_3^2 f_3} = f_i \left[\frac{(y_0(1-f_i) + y_1 f_1^* + y_2 f_2^* + y_3 f_3^*)^2}{y_0^2(1-f_i) + y_1^2 f_1^* + y_2^2 f_2^* + y_3^2 f_3^*} \right] = f_i a \quad (16)$$

where, by definition

$$f_0 + (f_1 + f_2 + f_3) = f_0 + f_i = 1 \quad (17)$$

$$f_1^* + f_2^* + f_3^* = 1 \quad (18)$$

The term inside the brackets of Eq. (16) is denoted a . The factor a approaches unity as f_i approaches 100% and the jet composition converges to a single ion species. In a rigorous calculation using the VDF throughout the plume, a may be evaluated using Eq. (19).

$$a = \frac{\Phi_{\text{VDF}}}{f_i} = \frac{1}{\dot{m} f_i} \frac{\left(\pi \int_{-\pi/2}^{\pi/2} \dot{m}(\theta) \sin(\theta) \bar{v}(\theta) d\theta \right)^2}{\left(\pi \int_{-\pi/2}^{\pi/2} \dot{m}(\theta) \sin(\theta) \bar{v}^2(\theta) d\theta \right)} \quad (19)$$

The factor a has a weak dependence on ionization fraction for $f_i > 0.70$, which is considered a lower limit on ionization fraction for the jet-mode Hall thruster operating regime. Experimental ion species compositions from numerous Hall thruster investigations were analyzed using the assumption of a trimodal ion population with delta function velocity distributions. For 100% ionization, a ranged from approximately 0.94-0.99, and is shifted upward 2-3% for $f_i = 0.70$.⁴⁶ The trimodal ion composition analysis established that a has an empirical dependence on average charge Q for delta function velocity distributions, which is expressed in Eq. (20) for calculation of a with

unknown ionization fraction. Uncertainty in the empirical linear relationship is conservatively estimated at $\pm 2\%$.

Further examination of a in Appendix A evaluates variations due to ionization fraction and ion species composition.

$$a \cong 1.14 - 0.13Q \quad (20)$$

where, average charge Q is defined by

$$Q = f_1^* + 2f_2^* + 3f_3^* \quad (21)$$

Evaluating Plume Divergence Losses in Propellant Utilization

The momentum weighted average plume divergence is defined in Eq. (22) as the ratio of axial momentum that produces thrust to the total momentum exhausted in the plume. Momentum losses associated with plume divergence may be calculated with knowledge of the input mass flow, measured thrust, and the mass weighted average velocity.

$$\Phi_{\text{DIV}} = \langle \cos(\theta) \rangle_{mv}^2 = \left(\frac{2\pi \int_{-\pi/2}^{\pi/2} \dot{m}(\theta) \bar{v}(\theta) \cos(\theta) \sin(\theta) d\theta}{2\pi \int_{-\pi/2}^{\pi/2} \dot{m}(\theta) \bar{v}(\theta) \sin(\theta) d\theta} \right)^2 = \left(\frac{\mathbf{T}}{\dot{m} \langle \bar{v} \rangle_m} \right)^2 \quad (22)$$

The value $\langle \cos(\theta) \rangle^2$ has been used in previous analyses to describe plume focusing^{28,29,30}, but there has not been a consistent method to calculate the effect of plume divergence on thrust. This is primarily due to the difficulty of measuring particle velocity throughout the plume. Charge divergence in the plume is indicative of off-axis velocity losses in thrust, and is a useful alternative for experimental characterization of performance losses due to plume divergence. The momentum weighted average divergence is approximated as the charge weighted average divergence in Eq. (23), which enables calculation of off-axis cosine losses in Eq. (24) using the ratio of axial beam current to total beam current as measured by a Faraday probe.

$$\langle \cos(\theta) \rangle_{mv}^2 = \left(\frac{2\pi \int_{-\pi/2}^{\pi/2} \left(\frac{\dot{m}(\theta) \bar{v}(\theta)}{j(\theta)} \right) j(\theta) \cos(\theta) \sin(\theta) d\theta}{2\pi \int_{-\pi/2}^{\pi/2} \left(\frac{\dot{m}(\theta) \bar{v}(\theta)}{j(\theta)} \right) j(\theta) \sin(\theta) d\theta} \right)^2 \cong \left(\frac{2\pi \int_{-\pi/2}^{\pi/2} j(\theta) \cos(\theta) \sin(\theta) d\theta}{2\pi \int_{-\pi/2}^{\pi/2} j(\theta) \sin(\theta) d\theta} \right)^2 = \langle \cos(\theta) \rangle_j^2 \quad (23)$$

$$\Phi_{\text{DIV}} \cong \langle \cos(\theta) \rangle_j^2 = \left(\frac{2\pi \int_{-\pi/2}^{\pi/2} j(\theta) \cos(\theta) \sin(\theta) d\theta}{2\pi \int_{-\pi/2}^{\pi/2} j(\theta) \sin(\theta) d\theta} \right)^2 = \left(\frac{I_{\text{Axial}}}{I_{\text{Beam}}} \right)^2 \quad (24)$$

Off-axis cosine losses integrated in the numerator of Eq. (24) quantify the axial beam current that generates thrust. This formulation creates a method where the plume vector loss is evaluated in a scalar form. The calculation of Φ_{DIV} is complicated by the presence of charge exchange in the plume, which causes artificial increases in measured beam current at high angles and artificially increases divergence losses.

The ratio $\dot{m}(\theta)\bar{\mathbf{v}}(\theta)/j(\theta)$ introduced in Eq. (23) reveals the difference between momentum divergence and charge divergence. This ratio is evaluated in Appendix B for variations in ionization fraction and ion species population. In Eq. (25), the ratio is evaluated at off-axis angle θ , and reduced to a function of Q , ΔV , f_i , \mathbf{y}_0 , and α .

$$\frac{\dot{m}(\theta)\bar{\mathbf{v}}(\theta)}{j(\theta)} = \left(2\Delta V \frac{M}{F} \right)^{1/2} \left[\left(\frac{a}{Q} \right)^{1/2} \left(\frac{y_0^2 (1-f_i)}{Q} + 1 \right)^{1/2} \right] \bigg|_0 = \left(2\Delta V \frac{M}{F} \right)^{1/2} \gamma \bigg|_0 \propto Q^{-1/2} \quad (25)$$

The term inside the brackets of Eq. (25) is denoted γ , and characterizes differences between momentum weighted divergence and charge weighted divergence. The factor γ is proportional to $Q^{-1/2}$, where spatial variation of average charge in the plume is the primary source of discrepancy between momentum weighted divergence and charge weighted divergence. Significant variations in average charge within the azimuthal region of highest beam current may alter plume divergence calculations by less than 3%. Secondary effects evident in Eq. (25) include ionization fraction and the role of average acceleration potential in momentum. Appendix B details the analysis used in Eq. (25) and illustrates variations due to ionization fraction and ion population.

Decoupling Voltage and Current Utilization

Energy efficiency is the ratio of jet kinetic energy to anode electrical energy, and is factored in Eq. (26) as the product of voltage utilization and current utilization. It is convenient to introduce χ , which is defined in Eq. (27) as the product of particle ionization fraction, f_i , and average ion charge, Q , for a plasma with three ion species. Although χ cancels in the energy efficiency term, it is shown in Equations (30) and (31) to reveal the physical nature of the voltage and current utilization inherent in the thrust efficiency.

$$\eta_{\text{energy}} = \frac{\frac{1}{2} \dot{m} \langle \bar{\mathbf{v}}^2 \rangle_m}{P_{\text{in}}} = \left[\frac{\langle \bar{\mathbf{v}}^2 \rangle_m}{\langle \bar{\mathbf{v}}_{\text{ions}}^2 \rangle_m} \frac{\frac{1}{2} \langle \bar{\mathbf{v}}_{\text{ions}}^2 \rangle_m}{\frac{F}{M} V_a} \right] \left[\frac{\dot{m}}{I_a} \frac{F}{M} \right] = [\chi (1-\beta)] \left[\frac{(1-r)}{\chi} \right] = (1-\beta)(1-r) \quad (26)$$

where, by definition

$$\chi = f_1 + 2f_2 + 3f_3 = f_i (f_1^* + 2f_2^* + 3f_3^*) = f_i Q \quad (27)$$

The ratio of average particle specific kinetic energy to average ion specific kinetic energy in Eq. (26), $\langle \bar{\mathbf{v}}^2 \rangle_m / \langle \bar{\mathbf{v}}_{\text{ions}}^2 \rangle_m$, is written in terms of f_i and reduced species mass fractions in Eq. (28).

$$\frac{\langle \bar{\mathbf{v}}^2 \rangle_m}{\langle \bar{\mathbf{v}}_{\text{ions}}^2 \rangle_m} = \frac{f_0 \mathbf{v}_0^2 + f_1 \mathbf{v}_1^2 + f_2 \mathbf{v}_2^2 + f_3 \mathbf{v}_3^2}{f_1 \mathbf{v}_1^2 + f_2 \mathbf{v}_2^2 + f_3 \mathbf{v}_3^2} = f_i \left[1 + \frac{\mathbf{y}_0^2 (1-f_i)}{f_1^* \mathbf{y}_1^2 + f_2^* \mathbf{y}_2^2 + f_3^* \mathbf{y}_3^2} \right] \approx f_i \quad (28)$$

The bracketed quantity in Eq. (28) is very close to unity under all reasonable conditions of Hall thruster operation due to the low value of \mathbf{y}_0 in the numerator, i.e., $\mathbf{y}_0^2(1-f_i) \approx 1 \times 10^{-4}$ for experimental estimates of $\mathbf{y}_0 \approx 0.03$.⁴² Thus, the approximation, $\langle \bar{\mathbf{v}}^2 \rangle_m / \langle \bar{\mathbf{v}}_{\text{ions}}^2 \rangle_m \approx f_i$ is accurate to better than one in ten thousand.

Equation (29) transforms the first term in brackets of Eq. (26) into an expression that contains explicit utilization of acceleration potential for each ion species, $\delta V_1/V_a$, $\delta V_2/V_a$, $\delta V_3/V_a$. An ExB probe measurement of reduced ion mass fractions and estimation of ion acceleration potentials would enable a voltage utilization to be calculated for each ion species, since the particle kinetic energy is proportional to charge and acceleration potential ($\frac{1}{2} \mathbf{v}_z^2 = z \delta V_z \mathcal{F}/M$).

$$\frac{\langle \bar{\mathbf{v}}^2 \rangle_m}{\langle \bar{\mathbf{v}}_{\text{ions}}^2 \rangle_m} \frac{\frac{1}{2} \langle \bar{\mathbf{v}}_{\text{ions}}^2 \rangle_m}{\frac{F}{M} V_a} = f_i \left(f_1^* \frac{\delta V_1}{V_a} + 2f_2^* \frac{\delta V_2}{V_a} + 3f_3^* \frac{\delta V_3}{V_a} \right) \quad (29)$$

To simplify the analysis, all ions are considered to be created in the same zone whose length is small compared to the acceleration length, such that $\Delta V = \delta V_1 = \delta V_2 = \delta V_3$. Previous investigations by Kim⁴³ and King⁴⁴ found that species dependent energy to charge ratios varied by tens of volts using different types of energy analyzers. This variation energy to charge ratio is less than 10% of the discharge voltage. According to Hofer⁴⁵, the

approximation will have a negligible effect on accuracy since the plume is predominantly composed of singly ionized xenon. Thus, the most probable ion acceleration potential, ΔV , as measured with a retarding potential analyzer (RPA) enables the first term in brackets of Eq. (26) to be expressed in terms of the average voltage utilization efficiency and χ in Eq. (30).

$$\frac{\langle \bar{v}^2 \rangle_m}{\langle \bar{v}_{ions}^2 \rangle_m} \frac{\frac{1}{2} \langle \bar{v}_{ions}^2 \rangle_m}{\frac{F}{M} V_a} = f_i \frac{\Delta V}{V_a} (f_1^* + 2f_2^* + 3f_3^*) = f_i (1-\beta) Q = (1-\beta) \chi \quad (30)$$

The average voltage utilization, $(1-\beta) = \Delta V/V_a$, compares the most probable potential gained by ions with the applied anode potential, and is unity for ionization at the anode face where ions are accelerated through the entire anode potential.

The second bracketed term in Eq. (26) is transformed in Eq. (31) into an expression containing the current utilization efficiency and χ .

$$\frac{\dot{m}}{I_a} \frac{F}{M} = \frac{\dot{m}(F/M)}{I_a} \frac{f_i Q}{f_i Q} = \frac{\dot{m}(F/M)}{I_a} \frac{\chi}{\chi} \frac{1}{\chi} = \frac{I_{Beam}}{I_a} \frac{1}{\chi} = \frac{(1-r)}{\chi} \quad (31)$$

Current utilization efficiency, $(1-r) = I_{Beam}/I_a$, is the fraction of cathode electron flow that electrically neutralizes the accelerated positive ions in the plume, and is defined as the ratio of ion beam current to discharge current. The total ion beam current exiting the thruster is given by $I_{Beam} = \chi \dot{m} (F/M)$.

Electrons recycled to the anode ionize neutral propellant and sustain dissipative plasma processes. The minimum power required to produce a given trimodal ion distribution is $\dot{m} f_i (\epsilon_1 f_1^* + \epsilon_2 f_2^* + \epsilon_3 f_3^*)$ such that the minimum recycled electron fraction required to sustain ionization may be expressed by Eq. (32).

$$r_{min} = \frac{\dot{m}}{I_a V_a} f_i (\epsilon_1 f_1^* + \epsilon_2 f_2^* + \epsilon_3 f_3^*) \quad (32)$$

Power from recycled electrons that is not used for ionization is lost by Joule heating and amounts to $(r-r_{min})I_a V_a$.

Combining the derivation of energy efficiency with propellant utilization efficiency in Eq. (33) yields two useful groups of experimental parameters, denoted E_1 and E_2 , which may be written using the preceding utilization efficiencies. The parameters are formed such that the product of E_1 and E_2 is equal to thruster efficiency. Equations (34) and (35) show how these quantities are calculated based solely on telemetry and thrust measurements, and

provide insight about the relative magnitudes of the individual utilization efficiencies in the absence of plume measurements.

$$\eta_{\text{thrust}} = \Phi \eta_{\text{energy}} = \Phi (1 - \beta) (1 - r) = [\Phi(1 - \beta)\chi] \left[\frac{(1 - r)}{\chi} \right] = E_1 E_2 \quad (33)$$

$$E_1 = \Phi(1 - \beta)\chi = \Phi_{\text{DIV}} (1 - \beta) a Q f_i^2 = \frac{\frac{1}{2} \left[\frac{\mathbf{T}}{\dot{m}} \right]^2}{V_a \frac{F}{M}} = \frac{\frac{1}{2} [\langle \bar{\mathbf{v}} \rangle_m \langle \cos(\theta) \rangle_{mv}]^2}{V_a \frac{F}{M}} \quad (34)$$

$$E_2 = \frac{(1 - r)}{\chi} = \frac{(1 - r)}{f_i Q} = \frac{\dot{m}}{I_a} \frac{F}{M} \quad (35)$$

For fixed thruster telemetry inputs V_a and \dot{m} , the dimensionless experimental parameters E_1 and E_2 separate changes in anode efficiency to processes related to variations in discharge current or thrust. The quantity $E_1 \sim T^2$, and is a function of propellant utilization, voltage utilization, and χ . Experimental parameter E_1 relates the applied acceleration potential to the jet vector properties. The quantity $E_2 \sim I_a^{-1}$, and is a function of current utilization and the χ . Experimental parameter E_2 relates the input mass flow to the flow of charge. The inverse of E_2 was developed in the Russian manual on stationary plasma engines in 1989, where it was defined as the exchange parameter.²⁸ The naming convention used here describes the exchange of applied input parameters to operational thruster properties. Thus, E_1 is appropriately termed the Voltage Exchange Parameter and E_2 is termed the Mass Exchange Parameter. While ionization and acceleration processes are closely coupled, the form of the experimental parameters indicates that propellant utilization and voltage utilization are principal in the formation of thrust. In the absence of diagnostics for the determination of plasma properties, these experimental parameter groups allow limits to be placed on acceptable values for the average charge Q , ionization fraction f_i , and momentum divergence loss Φ_{DIV} .^{46,47}

In the absence of thrust measurements, such as on-orbit applications, thrust may be estimated using telemetered beam voltage and beam current as shown in Eq. (36) and (37). This formulation is similar to the one dimensional analysis used to estimate thrust of the SERT-II ion engines, which is equivalent to Eq. (37) when χ and Φ are unity.^{48,49,50,51,52,53} An analogous expression was used to estimate thrust of the NSTAR ion engines on-board NASA's Deep Space 1 by including factors to account for multiply charged ions and beam cosine losses.⁵⁴ These

factors are based on the formulation of thrust by Masek *et al.* and are related to the ratio $(\Phi/\chi)^{1/2}$ as shown in Eq. (37).²¹

$$\mathbf{T} = \dot{m} \langle \bar{\mathbf{v}} \rangle_m \langle \cos(\theta) \rangle_{mv} = \dot{m} (\langle \bar{\mathbf{v}}^2 \rangle_m \Phi)^{1/2} \quad (36)$$

$$\mathbf{T} = \left(\frac{I_{\text{Beam}}}{\chi \frac{F}{M}} \right) \left(2 \frac{F}{M} V_a (1-\beta) \chi \Phi \right)^{1/2} = I_{\text{Beam}} (\Delta V)^{1/2} \left(\frac{2M}{F} \right)^{1/2} \left(\frac{\Phi}{\chi} \right)^{1/2} \quad (37)$$

Experimental Demonstration of Analytical Methodology

The efficiency analysis is demonstrated using experimental results from the NASA-173Mv2 laboratory model Hall thruster operating at 700 V and 10 mg/s.^{2,45,55} The investigation consisted of thrust measurements and examination of the ion voltage distribution, plasma potential, ion species composition, and ion current density in the far-field plume. Experimental results are listed in Table 1.

Calculated plasma properties in Table 2 show a high ionization fraction of ~98% and a large ion beam current. The backflow electron current not applied to beam neutralization is $r=0.19$, whereas the minimum recycled electron fraction required for propellant ionization is $r_{\text{min}}=0.02$ of the total discharge current. Losses due to Joule heating are estimated at $(r-r_{\text{min}})I_a V_a \approx 1100$ W, whereas the total energy losses are $(1-\eta_{\text{energy}})I_a V_a \approx 1500$ W of the total 6700 W discharge power.

Examination of the propellant utilization shows that plume divergence is a dominant performance loss mechanism for this operating condition. For $\Phi_{\text{DIV}}=0.88$, the charge weighted plume divergence is 20° , whereas the commonly reported 95% charge divergence half-angle is significantly higher at 39° . Losses due to non-uniformity of the VDF were minimal for $\Phi_{\text{VDF}}=0.97$, where the magnitude of α was estimated using the experimental ion species fractions with delta function velocity distributions.

Thruster utilization efficiencies and anode efficiency are shown in Table 3. Anode efficiency is calculated using two methods, (1) using measured thrust and telemetry and (2) using plume diagnostics. Both methods resulted in anode efficiency of 66%. The overall uncertainty in thruster efficiency based on thrust and telemetry data is 2%, whereas the uncertainty in efficiency using plasma diagnostics is ~15%.

The uncertainty in thrust and plume measurements were propagated into calculations of plasma properties and utilization efficiencies. Experimental errors associated with Faraday probe scans manifest in both current utilization and propellant utilization, and translate into a large degree of uncertainty when calculating thruster efficiency using plume diagnostics. As distance from the exit plane increases, charge exchange (CEX) collisions in the plume lead to a decrease in core ion beam current and an increase in computed beam divergence. These effects artificially decrease efficiency as calculated with plume diagnostics and increase measurement uncertainty. Near-field measurements close to the exit plane would minimize the effects of CEX collisions.

The far-field Faraday probe measurements on the NASA-173M2 were taken at 98.5 cm downstream of the exit plane, leading to estimated uncertainty in axial and total beam current of ~10%. If the uncertainty in calculated beam current calculations were reduced to 5%, the overall uncertainty in efficiency calculated with plume measurements would decrease from 15% to 8%. This highlights the importance of high fidelity measurements with minimal uncertainty for calculating plasma properties using the analytical technique.

Table 1: Thrust, Telemetry, and Far-field Plume Measurements

T [mN]	$298 \pm 1\%$
V_a [V]	$700.3 \pm 0.05\%$
I_a [A]	$9.62 \pm 0.2\%$
\dot{m} [mg/s]	$10.0 \pm 1\%$
f_1^*	0.92 ± 0.04
f_2^*	0.07 ± 0.02
f_3^*	0.01 ± 0.01
ΔV [V]	675 ± 10
I_{Beam} [A]	$7.8 \pm 10\%$
I_{Axial} [A]	$7.3 \pm 10\%$

Table 2: Calculated Plasma Properties

$\chi = I_b / (\dot{m} \mathcal{F}/M)$	$1.07 \pm 10\%$
$Q = f_1^* + 2f_2^* + 3f_3^*$	$1.09 \pm 3\%$
$f_i = \chi / Q$	$0.98 \pm 10\%$
$\alpha \approx (0.03(1-f_i) + f_1^* + \sqrt{2}f_2^* + \sqrt{3}f_3^*)^2 / (0.001(1-f_i) + Q)$	$0.99 \pm 2\%$
$\Phi_{VDF} = \alpha f_i$	$0.97 \pm 11\%$
$\Phi_{DIV} = (I_{Axial} / I_{Beam})^2$	$0.88 \pm 10\%$
$\lambda = \cos^{-1} \sqrt{\Phi_{DIV}}$	$20^\circ \pm 10\%$
95% Charge Divergence Half-Angle	$39^\circ \pm 10\%$
$r_{min} = \dot{m} f_i (\epsilon_1 f_1^* + \epsilon_2 f_2^* + \epsilon_3 f_3^*) / (V_a I_a)$	$0.02 \pm 11\%$

Table 3: Calculated Thrust Efficiency and Utilization Efficiencies

$E_1 = 1/2 (T / \dot{m})^2 / (V_a \mathcal{F} / M)$	$0.87 \pm 2\%$
$E_2 = (\dot{m} / I_a) (\mathcal{F} / M)$	$0.76 \pm 1\%$
$(1-\beta) = \Delta V / V_a$	$0.96 \pm 1\%$
$(1-r) = I_{Beam} / I_a$	$0.81 \pm 10\%$
$\eta_{energy} = (1-\beta) (1-r)$	$0.78 \pm 10\%$
$\Phi = \Phi_{VDF} \Phi_{DIV}$	$0.85 \pm 15\%$
$\eta_{thrust} = (1-\beta) (1-r) \Phi$ (Analytical)	$0.66 \pm 15\%$
$\eta_{thrust} = 1/2 T^2 / (\dot{m} V_a I_a)$ (Telemetry)	$0.66 \pm 2\%$

Summary

A standardized Hall thruster performance architecture was developed that factored anode efficiency as the product of terms representing the utilization of thruster input parameters, including: (1) voltage utilization, (2) current utilization, and (3) propellant utilization efficiency. The analysis decomposed anode efficiency from first principles, and formulated the relationship such that losses associated with energy conversion are analyzed separately from losses associated with jet vector properties. Energy efficiency encompassed performance losses resulting from Joule heating and ionization processes, and is defined as the product of current utilization and voltage utilization. Current utilization can never be unity due to a finite flow of electrons that are recycled to the anode to sustain ionization processes. Propellant utilization efficiency incorporates losses from plume divergence and the ion jet composition, and is unity for 100% ionization to a single ion species whose velocity vectors are directed along the same thrust axis. The momentum weighted divergence loss term ($\langle \cos(\theta) \rangle_{mv}^2$) in propellant utilization contains all jet vector losses. The proposed analysis is compared to past performance methodologies, with similarities to previous architectures formulated by Masek *et al.* in the ion engine community and Belan, Kim, Oranskiy, and Tikhonov from the Kharkov Aviation Institute.^{21,28}

A case study was presented with experimental performance and far-field plume measurements for a laboratory model Hall thruster. Thrust measurements resulted in anode efficiency of $66 \pm 2\%$, compared to $66 \pm 25\%$ when efficiency was calculated from plume measurements using the analytical model. The performance methodology reveals low current utilization and high plume divergence as the primary performance drivers for this operating condition. Although uncertainty associated with Faraday probe current density measurements in the jet were significant, the numerical agreement between the two techniques supports the proposed methodology. Fidelity of the performance architecture and the nature of analytical factorization permit the extraction of additional plasma parameters and the placement of bounding limits on discharge properties.

ACKNOWLEDGEMENT

The authors acknowledge numerous insightful discussions with Justin Koo, Brian Beal, Bryan Reid, and James Haas that contributed to development of the ideas and concepts presented in this paper.

APPENDIX A: The VDF Factor α for a Trimodal Ion Distribution

The Φ_{VDF} component of propellant utilization is often absent in textbook equations where scalar energy quantities are compared to squared vector momentum quantities, since $\Phi_{\text{VDF}} > 0.99$ for shifted Maxwellian distributions common to chemical propulsion jets. To illustrate the dependence of Φ on the properties of a jet with non-uniform velocity distribution, a simple trimodal ion distribution with neutral xenon is studied. Consider a jet that contains Xe^0 , Xe^{+1} , Xe^{+2} , and Xe^{+3} with mass fractions of f_0 , f_1 , f_2 , and f_3 , respectively, such that $f_0+f_1+f_2+f_3=1$. To further simplify, the velocity of neutrals and each ion species is approximated with a delta function distribution of velocities, specified by \mathbf{v}_0 , \mathbf{v}_1 , \mathbf{v}_2 , and \mathbf{v}_3 . This approximation will not significantly affect conclusions that would result from a more complicated model, since each ion species is created within a narrow zone in the channel and the plume is predominantly composed of Xe^{+1} ions. The term Φ_{VDF} is shown in Eq. (A-1) for a trimodal ion distribution, and the extension to include higher charge states is a simple exercise.

$$\Phi_{\text{VDF}} = \frac{\langle \bar{\mathbf{v}} \rangle_m^2}{\langle \bar{\mathbf{v}}^2 \rangle_m} = \frac{(\mathbf{v}_0 f_0 + \mathbf{v}_1 f_1 + \mathbf{v}_2 f_2 + \mathbf{v}_3 f_3)^2}{\mathbf{v}_0^2 f_0 + \mathbf{v}_1^2 f_1 + \mathbf{v}_2^2 f_2 + \mathbf{v}_3^2 f_3} \quad (\text{A-1})$$

For convenience and compact notation, the ion number fraction is defined by $f_i = f_1 + f_2 + f_3$, where $f_0 + f_i = 1$. Reduced number fractions are defined by $f_0^* = f_0/f_i$, $f_1^* = f_1/f_i$, $f_2^* = f_2/f_i$, and $f_3^* = f_3/f_i$, such that $f_1^* + f_2^* + f_3^* = 1$. Ratios of velocities of Xe^0 , Xe^{+1} , Xe^{+2} , and Xe^{+3} to the velocity magnitude of Xe^{+1} are defined by $\mathbf{y}_0 = \mathbf{v}_0/|\mathbf{v}_1|$, $\mathbf{y}_1 = \mathbf{v}_1/|\mathbf{v}_1|$, $\mathbf{y}_2 = \mathbf{v}_2/|\mathbf{v}_1|$, $\mathbf{y}_3 = \mathbf{v}_3/|\mathbf{v}_1|$. This enables Φ_{VDF} to be written in Eq. (A-2) as a function explicit in f_i and the reduced ion mass fractions f_1^* , f_2^* , and f_3^* .

$$\Phi_{\text{VDF}} = f_i \left[\frac{(\mathbf{y}_0(1-f_i) + \mathbf{y}_1 f_1^* + \mathbf{y}_2 f_2^* + \mathbf{y}_3 f_3^*)^2}{\mathbf{y}_0^2(1-f_i) + \mathbf{y}_1^2 f_1^* + \mathbf{y}_2^2 f_2^* + \mathbf{y}_3^2 f_3^*} \right] = f_i \alpha \quad (\text{A-2})$$

The term inside the brackets of Eq. (A-2) is denoted α for a trimodal ion composition. The factor α approaches unity as f_i approaches 100% and the jet composition converges to a single ion species. Figure A-1 shows the relationship between α and average ion charge, Q , for a trimodal ion population with 100% ionization.

Reduced ion mass fractions f_1^* , f_2^* , and f_3^* are determined from several experimental studies of the three ion species fractions, depicting a range of thrusters, facilities, and operating conditions.^{45,56,57,58,59,60} To illustrate the variation in a using Eq. (A-2), ion velocity ratios of each species are calculated for the idealized case of ion creation in the same zone whose length is small compared to the acceleration length. This approximation is consistent with measurements by Kim⁴³ and King⁴⁴, who found that species dependent energy to charge ratios varied by tens of volts using different types of energy analyzers. As pointed out by Hofer⁴⁵, this assumption will have a negligible effect on the ion velocity ratio estimates since the plume is predominantly composed of singly ionized xenon. Thus, the ion species kinetic energies are proportional to their charge, such that the velocity ratio magnitudes are $|y_1|=1$, $|y_2|=\sqrt{2}$, and $|y_3|=\sqrt{3}$. The velocity of neutrals is at least 30 times smaller than that of Xe^{+1} , resulting in $|y_0|\approx 0.03$.⁴²

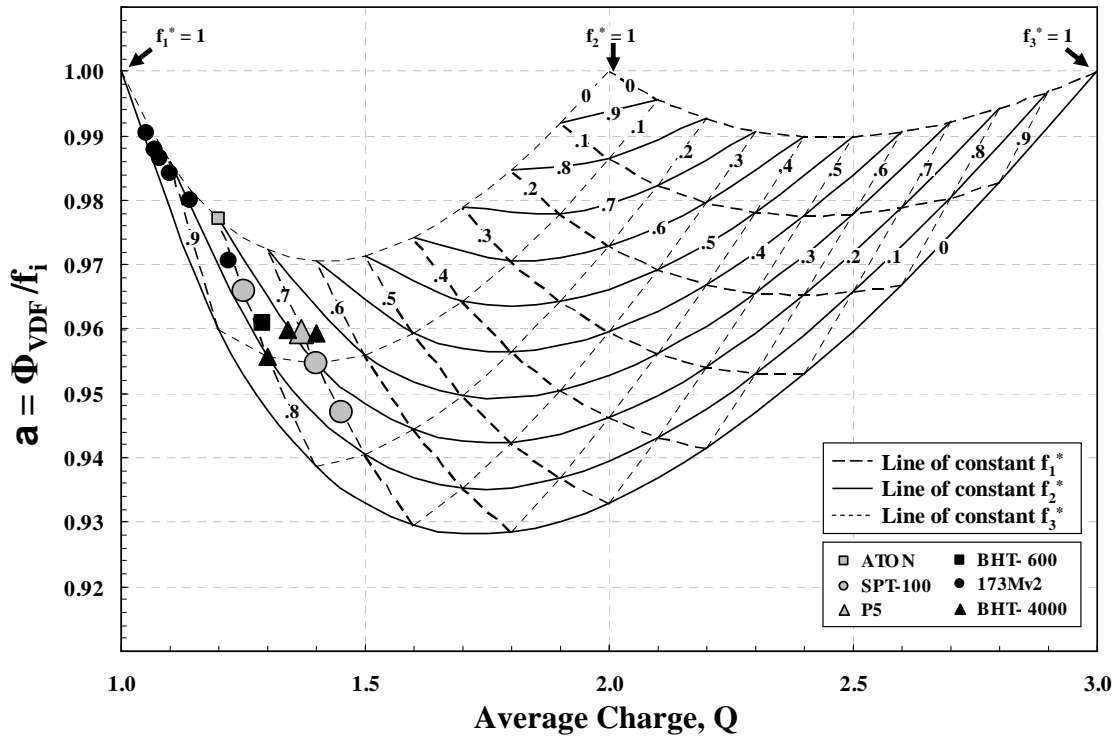


Fig. A-1 Dependence of a on plume ion composition. A complete set of constant f_1^* , f_2^* , f_3^* lines are shown for the $f_i = 1.0$ manifold. The factor a is calculated from ion species fractions reported in the Hall thruster literature for delta function velocity distributions, including: NASA-173Mv2 (2.5-9 kW)⁴⁵, ATON (~1 kW)⁵⁷, BHT-600 (0.6 kW)⁵⁷, SPT-100 (1.2 kW)⁵⁸, P5 (5 kW)⁵⁹, and the BHT-4000 (3 kW)⁶⁰.

The factor a has a weak dependence on ionization fraction for $f_i > 0.70$, which is considered a lower limit on ionization fraction for all jet-mode operating regimes. The non-linear sensitivity of a to ionization fraction is

illustrated in Figure A-2 for manifolds of $f_i=0.2$ and $f_i=1.0$. The region from $1.0 < Q < 1.5$ is shaded for $0.7 < f_i < 1.0$, which brackets the magnitude of a from 0.93 to 1.03 for most Hall thruster operation.

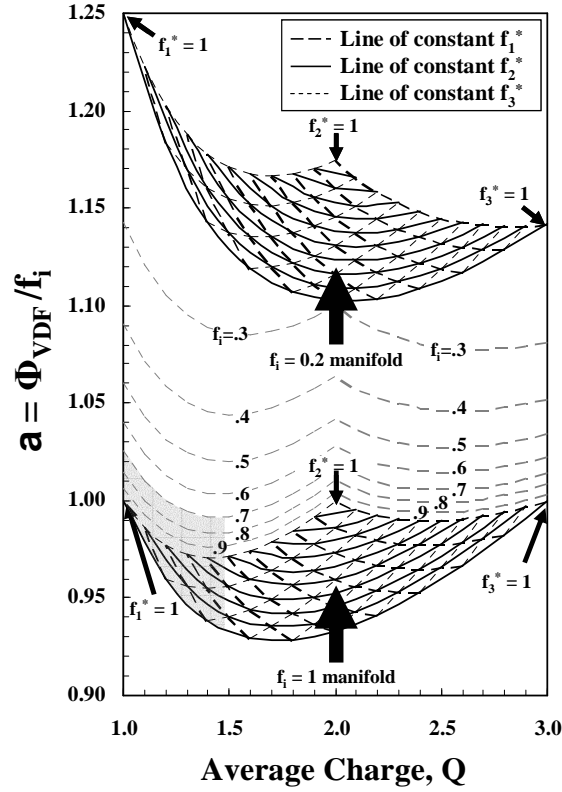


Fig. A-2 Variation in a due to ionization fraction, average charge, and ion species population for a trimodal ion composition with delta function velocity distributions. Ionization fraction manifolds are displayed for $f_i = 1.0$ and $f_i = 0.2$. Dashed lines of constant $f_1^* = 0$ and $f_3^* = 0$ are shown for $f_i = 0.9$ to 0.3 in increments of 0.1 .

The shaded region in Figure A-2 is magnified in Figure A-3, and the magnitude of a is evaluated for $0.7 < f_i < 1.0$ to illustrate the range of a for the survey of Hall thruster ion species compositions. For 100% ionization, a ranged from approximately 0.94-0.99, and is shifted upward 2-3% for $f_i=0.70$. The studies establish an empirical linear relationship between a on Q , which is expressed in Eq. (A-3). Uncertainty in a using the empirical relationship is conservatively estimated at $\pm 2\%$.

$$a \cong 1.14 - 0.13Q \quad (A-3)$$

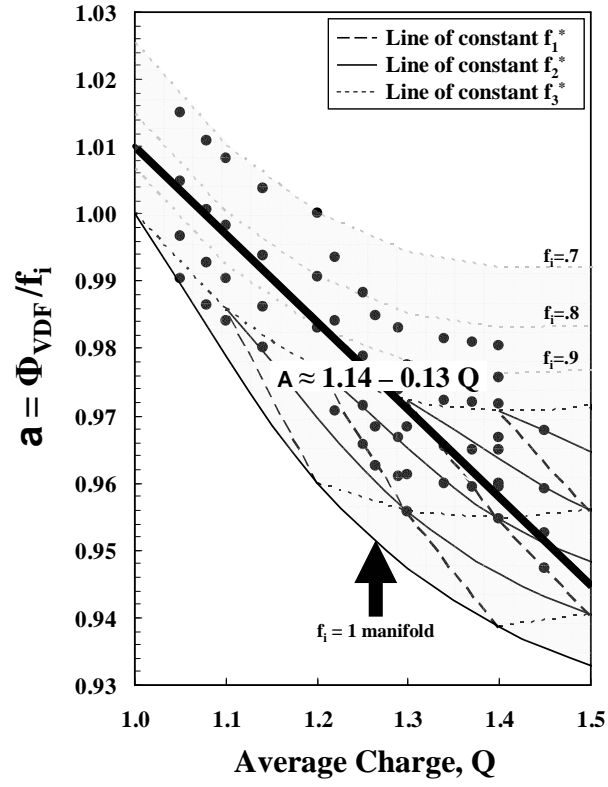


Fig. A-3 Range of a from the survey of Hall thruster ion species compositions for a trimodal ion population with delta function velocity distributions. The $f_i = 1.0$ manifold is displayed along with dashed lines of constant $f_3^* = 0$ for $f_i = 0.7, 0.8$, and 0.9 . The magnitudes of a are plotted for $f_i = 0.7, 0.8, 0.9$, and 1.0 .

APPENDIX B: The Divergence Factor γ for a Trimodal Ion Distribution

The momentum weighted average divergence is approximated as the charge weighted average divergence in Eq. (B-1), which enables calculation of off-axis cosine losses using the ratio of axial beam current to total beam current as measured by a Faraday probe.

$$\langle \cos(\theta) \rangle_{mv}^2 = \frac{\left(\frac{2\pi \int_{-\pi/2}^{\pi/2} \left(\frac{\dot{m}(\theta) \bar{v}(\theta)}{j(\theta)} \right) j(\theta) \cos(\theta) \sin(\theta) d\theta}{2\pi \int_{-\pi/2}^{\pi/2} \left(\frac{\dot{m}(\theta) \bar{v}(\theta)}{j(\theta)} \right) j(\theta) \sin(\theta) d\theta} \right)^2}{\left(\frac{2\pi \int_{-\pi/2}^{\pi/2} j(\theta) \cos(\theta) \sin(\theta) d\theta}{2\pi \int_{-\pi/2}^{\pi/2} j(\theta) \sin(\theta) d\theta} \right)^2} = \langle \cos(\theta) \rangle_j^2 \quad (\text{B-1})$$

Analysis of the ratio $\dot{m}(\theta)\bar{v}(\theta)/j(\theta)$ introduced in Eq. (B-1) characterizes the properties that cause differences between momentum weighted divergence and charge weighted divergence. Consider the trimodal ion jet from Appendix A with mass fractions of f_0 , f_1 , f_2 , and f_3 , respectively, such that $f_0+f_1+f_2+f_3 = f_0+f_1=1$. Reduced mass fractions are defined by $f_0^*=f_0/f_i$, $f_1^*=f_1/f_i$, $f_2^*=f_2/f_i$, and $f_3^*=f_3/f_i$, where $f_1^*+f_2^*+f_3^*=1$. Each particle species is approximated with a delta function velocity distribution and velocity ratios are calculated for the idealized case of ion creation at the same location, such that each ion is accelerated through the same potential. As a result, the ion species kinetic energies are proportional to their charge and the velocity ratio magnitudes are $|\mathbf{y}_1|=1$, $|\mathbf{y}_2|=\sqrt{2}$, and $|\mathbf{y}_3|=\sqrt{3}$. The ratio $\dot{m}(\theta)\bar{v}(\theta)/j(\theta)$ is evaluated at off-axis angle θ and formulated in terms of ΔV , Q , α , f_i , and \mathbf{y}_0 in Eq. (B-2), (B-3), (B-4), and (B-5).

$$\frac{\dot{m}(\theta)\bar{v}(\theta)}{j(\theta)} = \frac{\dot{m}(\theta)\bar{v}(\theta)}{\dot{m}(\theta)f_i(\theta)Q(\theta)\frac{F}{M}} = \frac{f_i\dot{m}(f_0^*\mathbf{y}_0 + f_1^*\mathbf{y}_1 + f_2^*\mathbf{y}_2 + f_3^*\mathbf{y}_3)}{f_i\dot{m}\frac{F}{M}(f_1^* + 2f_2^* + 3f_3^*)} \bigg|_{\theta} = |\mathbf{v}_1| \frac{M}{F} \left[\frac{f_0^*\mathbf{y}_0 + f_1^*\mathbf{y}_1 + f_2^*\mathbf{y}_2 + f_3^*\mathbf{y}_3}{(f_1^* + 2f_2^* + 3f_3^*)} \right] \bigg|_{\theta} \quad (\text{B-2})$$

$$\frac{\dot{m}(\theta)\bar{v}(\theta)}{j(\theta)} = |\mathbf{v}_1| \frac{M}{F} \left[\frac{\left((f_0^*\mathbf{y}_0 + f_1^*\mathbf{y}_1 + f_2^*\mathbf{y}_2 + f_3^*\mathbf{y}_3)^2 \right)^{1/2}}{\left(\mathbf{y}_0^2 f_0^* + \mathbf{y}_1^2 f_1^* + \mathbf{y}_2^2 f_2^* + \mathbf{y}_3^2 f_3^* \right)^{1/2}} \frac{1}{Q} \right] \bigg|_{\theta} \quad (\text{B-3})$$

$$\frac{\dot{m}(\theta)\bar{v}(\theta)}{j(\theta)} = |\mathbf{v}_1| \frac{M}{F} \left[\left(\frac{a}{Q} \right)^{1/2} \frac{\left(\mathbf{y}_0^2 (1-f_i) + f_1^* + 2f_2^* + 3f_3^* \right)^{1/2}}{Q} \right] \bigg|_{\theta} \quad (\text{B-4})$$

$$\frac{\dot{m}(\theta)\bar{v}(\theta)}{j(\theta)} = \left(2\Delta V \frac{M}{F} \right)^{1/2} \left[\left(\frac{a}{Q} \right)^{1/2} \left(\frac{\mathbf{y}_0^2 (1-f_i)}{Q} + 1 \right)^{1/2} \right] \bigg|_{\theta} = \left(2\Delta V \frac{M}{F} \right)^{1/2} \gamma \bigg|_{\theta} \quad (\text{B-5})$$

The term inside the brackets of Eq. (B-5) is denoted γ , and describes differences between momentum weighted divergence and charge weighted divergence associated with average charge Q , ionization fraction, and ion species population. The velocity ratio normalization term, $|\mathbf{v}_1|=(2 \Delta V \mathcal{F}/M)^{1/2}$, shows the momentum dependence on

acceleration potential. The quantity γ is further reduced in Eq. (B-6) and expressed in terms of Φ_{VDF} and χ . For experimental estimates of $|\mathbf{y}_0| \approx 0.03$,⁴² the value $\mathbf{y}_0^2(1-f_i) \approx 1 \times 10^{-4}$. Ionization fraction and ion species population are shown to have a negligible effect on γ in Figure B-1. Thus, the approximation $\gamma \approx (\alpha/Q)^{1/2}$ is better than one in ten thousand.

$$\gamma = \left(\frac{a}{Q} \right)^{1/2} \left(\frac{\mathbf{y}_0^2(1-f_i)}{Q} + 1 \right)^{1/2} \bigg|_{\theta} \approx \left(\frac{a}{Q} \right)^{1/2} = \left(\frac{\Phi_{\text{VDF}}}{\chi} \right)^{1/2} \bigg|_{\theta} \propto Q^{-1/2} \quad (\text{B-6})$$

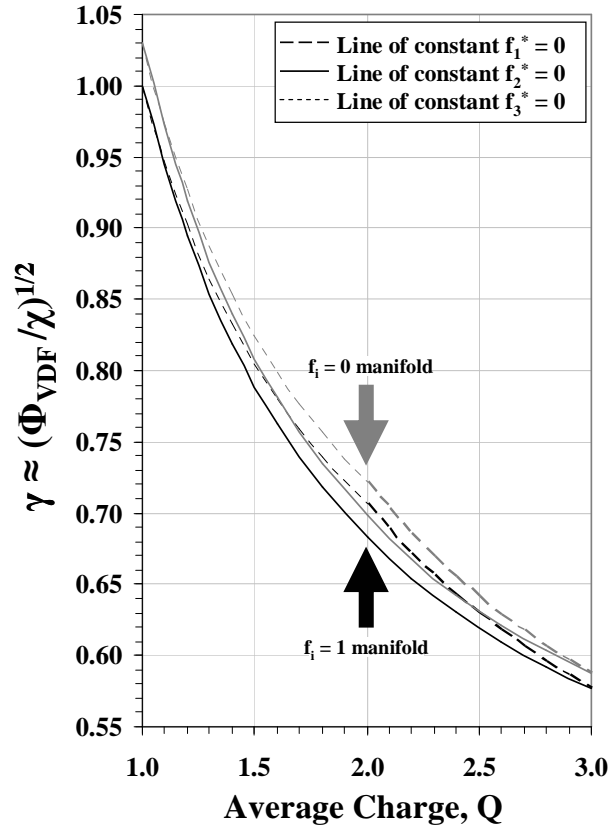


Fig. B-1 Variation in γ due to ionization fraction, average charge, and ion species population. Ionization fraction manifolds are shown for $f_i = 1.0$ and $f_i = 0$ with lines of constant $f_1^* = 0$, $f_2^* = 0$, and $f_3^* = 0$, and $f_3^* = 0$.

Variations in the magnitude of Q alter γ , but the azimuthal location of variations in Q is the dominant factor causing differences between momentum weighted divergence and charge weighted divergence. This effect is illustrated in Figure B-2, which shows a representative distribution of current density and beam current as a function of azimuthal position for a laboratory Hall thruster operating at 6 kW. The location of peak beam current in the plume is approximately 8 degrees from thruster centerline, and variations in Q within the azimuthal range of full

width half maximum (FWHM) will have the greatest effect on divergence. For the beam current in Figure B-2, this range is approximately ± 3 to ± 21 degrees. Near and far-field plume measurements of the SPT-100 and BHT-200 found that the ion species fraction did not significantly change within ± 15 degrees off thruster centerline, and the fraction of Xe^{+2} sharply increased by approximately 5% at ± 20 degrees.^{43,58,61} These changes in ion species fractions have a negligible effect on the value of $\langle \cos(\theta) \rangle_{mv}$, thus enabling the approximation of equivalence between momentum weighted divergence and charge weighted plume divergence as measured with a Faraday probe.

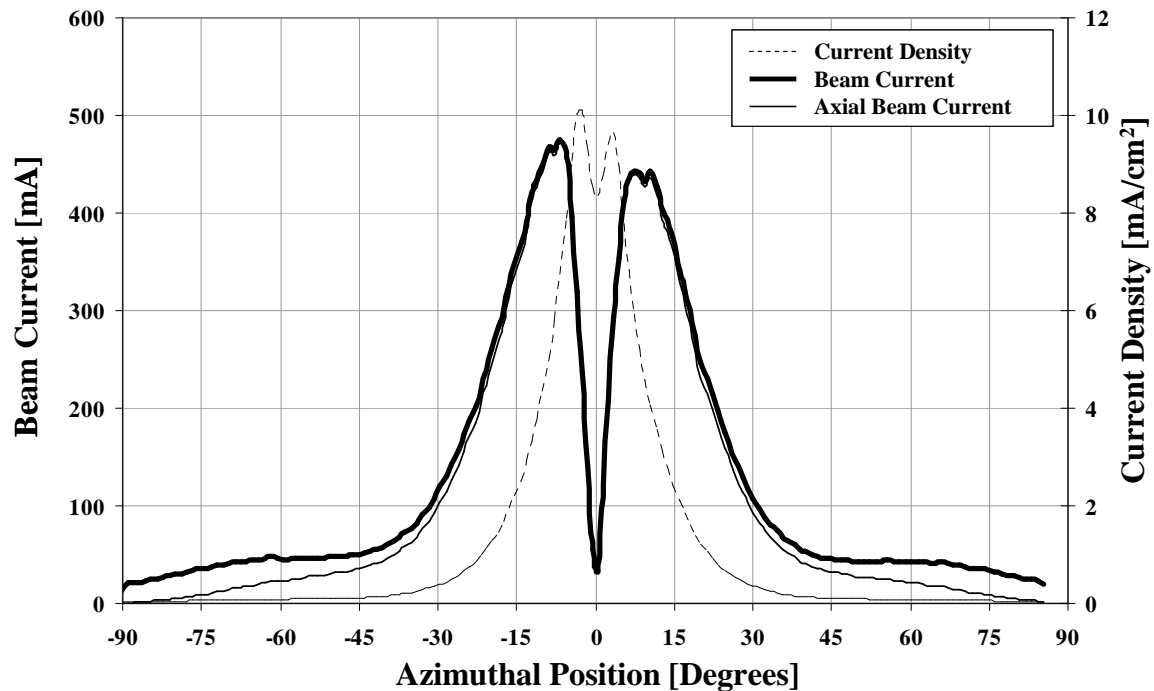


Fig. B-2 Distribution of beam current and current density at 1 meter radius as a function of azimuthal position in the plume of a laboratory Hall thruster operating at 6 kW.

REFERENCES

- ¹ Semenko, A., Kim, V., Gorshkov, O., Jankovsky, R., "Development of electric propulsion standards – current status and further activity," Proceedings of the 27th International Electric Propulsion Conference, Pasadena, CA, 15-19 October, 2001, Paper No. IEPC-2001-70.
- ² Hofer, R. R., and Gallimore, A.D., "High-specific impulse Hall Thrusters, Part 2: Efficiency Analysis," *Journal of Propulsion and Power*, Vol. 22, No. 4, 2006, pp. 732-740.
- ³ Linnell, J. A., Gallimore, A. D., "Efficiency Analysis of a Hall Thruster Operating with Krypton and Xenon," *Journal of Propulsion and Power*, Vol. 22, No. 6, 2006, pg. 1402-1418.
- ⁴ Fife, J. M., Martinez-Sanchez, M., "Two-Dimensional Hybrid Particle-In-Cell Modeling of Hall Thrusters," IEPC-95-240, Proceedings of the 24th International Electric Propulsion Conference, Moscow, Russia, 19-23 September 1995.

- ⁵ Hruby, V., Monheiser, J., Pote, B., Rostler, P., Kolencik, J., and Freeman, C., "Development of low power Hall thrusters," 30th Plasmadynamics and Lasers Conference, 28 June – 1 July, 1999, Norfolk, VA, Paper No. AIAA 1999-3534.
- ⁶ Morozov, A. I., "About Plasma Acceleration by Magnetic Fields," *Journal of Experimental and Theoretical Physics*, Vol. 32, N2, pp. 305, 1957 (In Russian).
- ⁷ Yushmanov, E. E., *Radial Distribution of the Potential in Cylindrical Trap with Magnetron Ion Injection*, In Book: *Plasma Physics and the Problem of Controlled Fusion*, M. A. Leontovich, Ed. Moscow, USSR: USSR Academy of Science, 1958, vol. 4, (In Russian).
- ⁸ Zharinov, A. V., "Electric Double Layer in Strong Magnetic Field," Kurchatov Inst. Rep., Moscow, USSR, 1961 (In Russian).
- ⁹ Lary, E.C., Meyerand, R. G. Jr., Salz, F., "Ion Acceleration in a gyro-dominated neutral plasma: Theory and experiment," *Bulletin of the American Physical Society*, Vol. 7, pg. 441, July 1962.
- ¹⁰ Seikel, G. R., Reshotko, E., "Hall-current Ion Accelerator," *Bulletin of the American Physical Society*, Vol. 7, pg. 414, July 1962.
- ¹¹ Janes, G. S., Dotson, J., Wilson, T., "Electrostatic Acceleration of Neutral Plasmas – Momentum Transfer Through Magnetic Fields," Proceedings of the Third Symposium on Advanced Propulsion Concepts (Gordon and Breach Science Publishers, Inc., New York, 1963), pg. 153 – 175.
- ¹² Brown, C. O., Pinsley, E. A., "Further Experimental Investigations of a Cesium Hall-Current Accelerator," *AIAA Journal*, Vol. 3, No. 5, 1965, pp. 853-859.
- ¹³ Morozov, A. I., "Investigation of the stationary electromagnetic plasma acceleration" – Doctoral Thesis, Institute of Atomic Energy named after I. V. Kurchatov, Moscow, 1965 (In Russian).
- ¹⁴ Janes, G. S., Lowder, R. S., "Anomalous Electron Diffusion and Ion Acceleration in a Low-Density Plasma", *Physics of Fluids*, Vol. 9, No. 6, 1966.
- ¹⁵ Zharinov, A. V., Popov, Y. S., "Acceleration of plasma by a closed Hall current," *Soviet Physics – Technical Physics*, Vol. 12, No. 2, August 1967, p. 208-211 (In Russian).
- ¹⁶ Morozov, A. I., "Effect of Near-wall Conductivity in Magnetized Plasma," *Journal of Applied Math Technical Physics*, Vol. 3, pg. 19-22, 1968 (In Russian).
- ¹⁷ Kaufman, H. R., "Technology of Closed-Drift Thrusters," *AIAA Journal*, Vol. 23, No. 1, 1985, pp. 78-87.
- ¹⁸ Zhurin, V. V., Kaufman, H. R., and Robinson, R. S., "Physics of closed drift thrusters," *Plasma Sources Sci. Technol.*, Vol. 8, 1999, pp. R1-R20.
- ¹⁹ Morozov, A. I., "The Conceptual Development of Stationary Plasma Thrusters", *Plasma Physics Reports*, Vol. 29, No. 3, pg. 235-250, 2003 (Translated from *Fizika Plazmy*, Vol. 29, No. 3, pg. 261-276, 2003)
- ²⁰ Kim, V., "History of the Hall Thrusters Development in USSR", Proceedings of the 30th International Electric Propulsion Conference, Florence, Italy, 17-20 September 2007, Paper No. IEPC-2007-142.
- ²¹ Masek, T. D., Ward, J. W., Kami, S., "Primary Electric Propulsion Thrust Subsystem Definition," AIAA 11th Electric Propulsion Conference and Exhibit, 19-21 March 1975, New Orleans, LA, Paper No. AIAA 75-405.
- ²² Brophy, J. R., "Stationary Plasma Thruster Evaluation in Russia", JPL Publication 92-4, NASA-CR-192823, March 15, 1992.
- ²³ Garner, C. E., Brophy, J. R., Polk, J. E., Semenko, S., Garkusha, V., Tverdokhlebov, S., Marrese, C., "Experimental Evaluation of Russian Anode Layer Thrusters," 30th AIAA/ASME/SAE/ASEE Joint Propulsion Conference, 27-29 June, 1994, Indianapolis, IN, Paper No. AIAA 1994-3010.
- ²⁴ Meyer, R. M., Manzella, D. H., "SPT Thruster Plume Characteristics", Proceedings of the 23rd International Electric Propulsion Conference, Seattle, WA, 13-16 September 1993, IEPC-93-096.
- ²⁵ Sankovic, J. M., Hamley, J. A., Haag, T. W., "Performance Evaluation of the Russian SPT-100 Thruster at NASA LeRC", IEPC-93-094, Proceedings of the 23rd International Electric Propulsion Conference, Seattle, WA, 13-16 September 1993, Paper No. IEPC-93-094.
- ²⁶ Garner, C. E., Polk, J. E., Goodfellow, K. D., Brophy, J. R., "Performance Evaluation on Life Testing of the SPT-100," Proceedings of the 23rd International Electric Propulsion Conference, Seattle, WA, 13-16 September 1993, Paper No. IEPC-93-091.
- ²⁷ King, L. B., Gallimore, A. D., Marrese, C. M., "Transport-Property Measurements in the Plume of an SPT-100 Hall Thruster," *Journal of Propulsion and Power*, Vol. 14, No. 3, 1998, pg. 327-335.
- ²⁸ Belan, N. V., Kim, V. P., Oransky, A. I., Tikhonov, V. B., *Stationary Plasma Engines*, Khar'kov Karh'kovskiy Aviatsonnyy Institut, 1989, pp. 164 - 166. (in Russian)
- ²⁹ Bugrova, A. I., Kim, V. P., Maslennikov, N. A., Morozov, A. I., "Physical Properties and Characteristics of Stationary Plasma Thrusters with Closed Electron Drift", Proceedings of the 22nd International Electric Propulsion Conference, Viareggio, Italy, 1991, Paper No. IEPC 91-079.
- ³⁰ Kim, V., "Main Physical Features and Processes Determining the Performance of Stationary Plasma Thrusters", *Journal of Propulsion and Power*, Vol. 14, No. 5, September – October, 1998.
- ³¹ Morozov, A. I., Bugrova, A. I., Desyatskov, A. V., Ermakov, Y. A., Kozintseva, M. V., Lipatov, A. S., Pushkin, A. A., Khartchevnikov, V. K., Churbanov, D. V., "ATON-Thruster Plasma Accelerator," *Plasma Physics Reports*, Vol. 23, No. 7, pp. 587-597, 1997 (Translated from *Fizika Plazmy*, Vol. 23, No. 7, pg. 635-645, 1997)
- ³² Bugrova, A. I., Lipatov, A. S., Morozov, A. I., Baranov, S. V., "Effect of the Ratio of Differently Charged Ions on the Integral Parameters of Stationary Plasma Thrusters of the ATON Type," *Technical Physics Letters*, Vol. 31, No. 11, pp. 943-946, 2005 (Translated from *Pis'ma v Zhurnal Tekhnicheskoi Fiziki*, Vol. 31, No. 21, pg. 87-94, 2005)

- ³³ Bouchoule, A., Boeuf, J. P., Heron, A., Duchemin, O., "Physical Investigations and Developments of Hall Plasma Thrusters", *Plasma Physics and Controlled Fusion*, 46 (2004), B407-B421.
- ³⁴ Ross, Jerry L., and King, Lyon B., "Ionization efficiency in electric propulsion devices," Proceedings of the 30th International Electric Propulsion Conference, Florence, Italy, 17-20 September 2007, Paper No. IEPC-2007-260.
- ³⁵ Sasoh, A., "Generalized Hall Acceleration," *Journal of Propulsion and Power*, Vol. 10, No. 2, 1994, pp. 251-254.
- ³⁶ Bober, A., "Numerical Analysis of Hall Thruster Firing Tests," *Journal of Propulsion and Power*, Vol. 23, No. 3, May-June 2007, pp. 537-543.
- ³⁷ Raites, Y., Fisch, N. J., "Parametric Investigations of a Nonconventional Hall Thruster," *Physics of Plasmas*, Vol. 8, No. 5, pg. 2579-2586, 2001.
- ³⁸ Grishin, S. D., Leskov, L. V., *Electrical Rocket Engines of Space Vehicles*, Publishing House "Mashinostroyeniye", Moscow, 1989, pp. 12.
- ³⁹ Raites, Y., Ashkenazy, J., and Guelman, M., "Propellant Utilization in Hall Thrusters," *Journal of Propulsion and Power*, Vol. 14, No. 2, 1998, pp. 247-253.
- ⁴⁰ Jameson, K. K., Goebel, D. M., Hofer, R. R., Watkins, R. M., "Cathode coupling in Hall Thrusters," Proceedings of the 30th International Electric Propulsion Conference, Florence, Italy, 17-20 September 2007, Paper No. IEPC-2007-278.
- ⁴¹ Hofer, R. R., Haas, J. M., Gallimore, A. D., "Ion Voltage Diagnostics in the Far-Field Plume of a High-Specific Impulse Hall Thruster," 39th AIAA/ASME/SAE/ASEE Joint Propulsion Conference and Exhibit, 20-23 July 2003, Huntsville, AL, Paper No. AIAA-2003-4556.
- ⁴² Hargus, W. A. Jr., Cappelli, M. A., "Interior and Exterior Laser-Induced Fluorescence and Plasma Measurements within a Hall Thruster," *Journal of Propulsion and Power*, Vol. 18, No. 1, 2002, pp. 159-168.
- ⁴³ Kim, S. W., Gallimore, A. D., "Plume Study of a 1.35-kW SPT-100 Using an ExB Probe," *Journal of Spacecraft and Rockets*, Vol. 39, No. 6, 2002, pp. 904-909.
- ⁴⁴ King, L. B., "Transport-property and mass spectral measurements in the exhaust plume of a Hall effect space propulsion system," PhD Dissertation, University of Michigan, Ann Arbor, MI, 1998.
- ⁴⁵ Hofer, R. R., "Development and Characterization of High-Efficiency, High Specific Impulse Xenon Hall Thrusters," PhD Dissertation, University of Michigan, Ann Arbor, Michigan. Published as NASA/CR-2004-213099, Glenn Research Center, June 2004.
- ⁴⁶ Larson, C. William, Brown, Daniel L., and Hargus, William A. Jr., "Thrust efficiency, energy efficiency and the role of the VDF in Hall thruster performance analysis," 43rd AIAA/ASME/SAE/ASEE Joint Propulsion Conference and Exhibit, 8-11 July 2007, Cincinnati, OH, Paper No. AIAA 2007-5270.
- ⁴⁷ Brown, Daniel L., Larson, C. William, Haas, James M., and Gallimore, Alec D., "Analytical extraction of plasma properties using a Hall thruster efficiency architecture," Proceedings of the 30th International Electric Propulsion Conference, Florence, Italy, 17-20 September 2007, Paper No. IEPC-2007-188.
- ⁴⁸ Mirels, H., Rosenbaum, B. M., "Analysis of One-Dimensional Ion Rocket," NASA TN D-266, 1960.
- ⁴⁹ Kaufman, H. R., "One-Dimensional Analysis of Ion Rockets," NASA TN D-261, 1960.
- ⁵⁰ Byers, D. C., "Angular Distribution of Kaufman Ion Thruster Beams," NASA TN D-5844, 1970.
- ⁵¹ Nieberding, W. C., Lesco, D. J., Berkopce, F. D., "Comparative In-Flight Thrust Measurements of the SERT II Ion Thruster," AIAA 8th Electric Propulsion Conference and Exhibit, August 31 – September 2, 1970, Stanford, CA, Paper No. AIAA 75-405.
- ⁵² Kerslake, W. R., Goldman, R. G., Nieberding, W. C., "SERT II: Mission, Thruster Performance, and In-Flight Thrust Measurements," *Journal of Spacecraft*, Vol. 8, No. 3, March 1971, pp. 213-224.
- ⁵³ Banks, B., Rawlin, V., Weigand, A., Walker, J., "Direct Thrust Measurement of a 30-cm Ion Thruster," NASA TM X-71646.
- ⁵⁴ Brophy, J. R., "NASA's Deep Space 1 Ion Engine (plenary)," *Review of Scientific Instruments*, Vol. 73, No. 2, Feb. 2002, pp. 1071-1078.
- ⁵⁵ Hofer, R. R., Jankovsky, R. S., Gallimore, A.D., "High-specific impulse Hall Thrusters, Part 1: Influence of Current Density and Magnetic Field," *Journal of Propulsion and Power*, Vol. 22, No. 4, 2006, pp. 721-731.
- ⁵⁶ Bugrova, A. I., Lipatov, A. S., Morozov, A. I., and Baranov, S. V., "Effect of the ratio of differently charged ions on the integral parameters of stationary plasma thrusters of the ATON type," *Technical Physics Letters*, Vol 31(11) 2005 pp 943-946
- ⁵⁷ Ekholm, J. M., Hargus, W. A., Larson, C. W., Nakles, M. R., and Reed, G., "Plume Characteristics of the Busek 600 W Hall Thruster," 42nd AIAA/ASME/SAE/ASEE Joint Propulsion Conference and Exhibit, 9-12 July 2006, Sacramento, CA, Paper No. AIAA-2006-4659.
- ⁵⁸ Kim, S. W., "Experimental Investigations of Plasma Parameters and Species-Dependent Ion Energy Distribution in the Plasma Exhaust Plume of a Hall Thruster," PhD Dissertation, University of Michigan, Ann Arbor, MI, 1999.
- ⁵⁹ Gulczynski, F. S., and Gallimore, A. D., "Near-field ion energy and species measurements of a 5-kW Hall Thruster," *Journal of Propulsion and Power*, Vol. 17, No. 2, 2001, pp. 418-427.
- ⁶⁰ Pollard, J. E., Diamant, K. D. Khayms, V., Werthman, L., King, D. Q., and de Grys, K. H., "Ion flux, energy, and charge-state measurements for the BPT-4000 Hall Thruster," 37th AIAA/ASME/SAE/ASEE Joint Propulsion Conference and Exhibit, Salt Lake City, Utah, Paper no. AIAA-2001-3351.
- ⁶¹ Beal, B. E., "Clustering of Hall Effect Thrusters for High Power Electric Propulsion Applications," PhD Dissertation, University of Michigan, Ann Arbor, Michigan, 2004.